Published in final edited form as:
Cancer Res. 2009 April 1; 69(7): 2838–2844. doi:10.1158/0008-5472.CAN-08-1397.

RhoGDI2 suppresses metastasis via unconventional regulation of RhoGTPases

Konstadinos Moissoglu[1], **Kevin S. McRoberts**[2], **Jeremy A. Meier**[1], **Dan Theodorescu**[1,2,4], and **Martin A. Schwartz**[1,3,4]

1*Robert M. Berne Cardiovascular Research Center, University of Virginia, Charlottesville, VA 22908, USA.*

2*Departments of Urology and Molecular Physiology and Biological Physics, University of Virginia, Charlottesville, VA 22908, USA.*

3*Departments of Microbiology, Cell Biology and Biomedical Engineering, University of Virginia, Charlottesville, VA 22908, USA.*

4*Mellon Urologic Cancer Research Institute, University of Virginia, Charlottesville, VA 22908, USA.*

Abstract

RhoGDI2 has been identified as a metastasis suppressor in bladder and possibly other cancers (1). This protein is a member of a family of proteins that maintain Rho GTPases in the cytoplasm and inhibit their activation and function. To understand the mechanism of metastasis suppression, we compared effects of RhoGDI1 and 2. Despite showing much stronger inhibition of metastasis, RhoGDI2 is a weak inhibitor of Rho GTPase membrane targeting and function. However, point mutants that increase or decrease the affinity of RhoGDI2 for GTPases abolished its ability to inhibit metastasis. Surprisingly, metastasis suppression correlates with increased rather than decreased Rac1 activity. These data show that RhoGDI2 metastasis inhibition works through Rho GTPases but via a mechanism distinct from inhibition of membrane association.

Keywords

bladder cancer; Rho GTPase; metastasis; RhoGDI; Rac

INTRODUCTION

RhoGDI2 was recently shown to function as a metastasis suppressor in bladder cancer and possibly other tumors (reviewed in (2)). Loss of RhoGDI2 expression strongly correlates with cancer stage, grade and the development of clinical metastasis in patients. Loss of RhoGDI2 also correlates with experimental metastasis in mouse models. Re-expression of RhoGDI2 in metastatic tumor lines inhibits experimental metastasis in these models without affecting primary tumor growth or growth rate in vitro.

Rho GDP dissociation inhibitor 2 (RhoGDI2 or GDI2) is a member of a small family of chaperone proteins, including RhoGDI1 and 3, that control Rho GTPases (3,4). Whereas GDI1 is ubiquitous, GDI2 is expressed mainly in hematopoietic, endothelial and urothelial cells (5). The Rho proteins Rho, Rac and Cdc42 that bind GDIs regulate many cellular functions, including cell polarity, migration, cell cycle progression, apoptosis, gene expression, vesicular

Correspondence should be addressed to Martin A. Schwartz: E-mail: maschwartz@virginia.edu Robert M. Berne Cardiovascular Research Center, University of Virginia, 415 Lane Road, MR5 Bldg., Room G111, Charlottesville, VA 22908, Phone: (434)243-4813.

trafficking and cancer. Rho GTPases cycle between an inactive (GDP-bound) state that is mainly cytosolic and an active (GTP-bound) state that is mainly membrane bound. Membrane targeting is predominantly mediated by carboxy-terminal sequences that include a geranyl-geranyl modification and a polybasic motif. The GDIs bind and sequester this hydrophobic moiety and are required to maintain Rho GTPases in the cytoplasm. They also inhibit activation by GEFs and inactivation by intrinsic and GAP-catalyzed GTP hydrolysis (6,7). Overexpression of GDI1 causes movement of Rho, Rac and Cdc42 into the cytoplasm and inhibits their activation and function (8–12). Conversely, depletion of GDI1 increases membrane association and activation of Rho GTPases (12–14).

Here, we set out to investigate the mechanism of tumor suppression by RhoGDI2. Based on behavior of GDI1, we anticipated that tumor suppression would be linked to inhibition of Rho GTPase function. Our data unexpectedly exclude such a mechanism and instead show that GDI2 activates its main target Rac.

MATERIALS AND METHODS

Cell culture and transfection

UMUC3 cells were grown in MEM supplemented with 10% fetal bovine serum, 1mM sodium pyruvate, penicillin and streptomycin (Invitrogen, Carlsbad, CA). T24 cells were grown in DMEM/F12 supplemented with 5% fetal bovine serum, penicillin and streptomycin. DNA plasmids were transfected with Effectene according to the manufacturer's instructions (Qiagen, San Diego, CA). Cells were analyzed for protein 24 h after transfection. For generation of stable GFP-RhoGDI-expressing UMUC3 cells, GFP-RhoGDI constructs were transfected together with pBABE-puro (15) at a 5:1 ratio. Polyclonal populations were obtained after selection with 2μg/ml puromycin, followed by FACS® sorting (Flow Cytometry Core Facility, University of Virginia). For RNAi experiments, T24 cells were transfected with pSuper.retro.puro-based constructs and clones were obtained following selection with puromycin (2μg/ml).

DNA plasmids and constructs

pcDNA3.1(+)-based plasmids containing RhoGDI1 or RhoGDI2 were used as templates for PCR amplification of the coding sequences that were subsequently subcloned into pEGFP-C1 to generate the corresponding GFP fusion proteins. The N174I, I177N and D182R mutations were introduced using the QuikChange® II Site-Directed Mutagenesis kit (Stratagene, La Jolla, CA). To generate FLAG-Rac, the coding sequence of human Rac was PCR-amplified and subcloned into pFLAG-CMV-4 (Sigma-Aldrich, St. Louis, MO). For RNAi experiments, duplexed oligos containing a sequence corresponding to nucleotides 97–116 in the coding region of human RhoGDI1 (5'-AAGAGCATCCAGGAGATCCA-3') or 123–141 of RhoGDI2 (5'-TGATGAGAGTCTAATTAAG-3') or control (mismatch) sequence were subcloned in pSuper.retro.puro (OligoEngine, Seattle, WA).

Immunoprecipitation and Western blotting

Stable UMUC3 cells that had been transfected with pFLAG-CMV-4-Rac were extracted in buffer containing 10mM Tris-HCl pH 7.4, 150mM NaCl, 1% NP-40, 8% glycerol and protease inhibitor cocktail, and immunoprecipitated with the anti-FLAG® M2 Affinity gel (Sigma) for 2 h at 4°C. Immobilized FLAG-Rac complexes were eluted using 0.2mg/ml 3x FLAG peptide. Samples were separated by SDS-PAGE, electrophoretically transferred to nitrocellulose (Bio-Rad Laboratories, Hercules, CA) and immunoblotted with the following primary antibodies: B-2 monoclonal anti-GFP (1/1,000; Santa Cruz Biotechnology), monoclonal anti-RhoGDI (1/5,000; clone 16; BD Transduction Laboratories, San Jose, CA), polyclonal anti-D4-GDI (1/1,000; Spring Bioscience, Fremont, CA), AC-40 monoclonal anti-actin (1/1,000; Sigma),

E7 monoclonal anti-beta tubulin (1/1,000; Developmental Studies Hybridoma Bank), 23A8 monoclonal anti-Rac1 (1/1,000; Millipore, Billerica, MA), monoclonal anti-Cdc42 (clone 44; 1/500; BD Transduction Laboratories, San Jose, CA), 26C4 monoclonal anti-RhoA (1/500; Santa Cruz Biotechnology), monoclonal anti-RhoA (1/250; Cytoskeleton, Inc.), anti-FLAG M2® monoclonal (1/5,000; Sigma), polyclonal anti-Erk1/2 (1/1,000; Cell Signaling Technology), polyclonal anti-phospho-SAPK/JNK (Thr183/Tyr185; 1/1,000; Cell Signaling Technology), polyclonal anti-SAPK/JNK (1/1,000; Cell Signaling Technology), polyclonal anti-phospho-PAK (Ser141; 1/1,000; Invitrogen), polyclonal anti-PAK (1/1,000; Santa Cruz Biotechnology) and polyclonal R18 anti-integrin β1 (gift of A. F. Horwitz, University of Virginia, Charlottesville, VA). Blots were washed and probed with secondary antibodies (horseradish peroxidase–conjugated anti-mouse or anti-rabbit immunoglobulin) followed by ECL substrate (Amersham Biosciences). Densitometric analysis was performed with Image J software.

Subcellular fractionation

Cells were washed with ice cold phosphate-buffered saline, scraped and homogenized in buffer containing 10 mM Tris-HCl pH 7.5, 5 mM $MgCl_2$, 1 mM DTT, 0.25 M sucrose and protease inhibitor cocktail (Sigma, St. Louis, MO). Nuclei and unbroken cells were removed by centrifugation at 1,000 × g for 10 min at 4°C, and the post-nuclear supernatant was centrifuged at 100,000 × g for 1 h at 4°C to separate the cytosolic and particulate fractions.

Pull-down assays

Cells were washed with ice-cold Tris-buffered saline (TBS) and lysed in buffer containing 50mM Tris pH 7.4, 500mM NaCl, 10mM $MgCl_2$, 1% Triton X-100, 0.1% SDS, 0.5% sodium deoxycholate and protease inhibitor cocktail (Sigma). Clarified lysates were then incubated with 20μg of recombinant GST-PBD or GST-RBD and Glutathione-Sepharose 4B beads (Amersham Biosciences) for 30 min at 4°C. Beads were washed with lysis buffer, eluted with sample buffer and analyzed by immunoblotting.

In vitro growth, subcutaneous tumorigenicity and experimental metastasis

Cells (10^5) were seeded onto 6-well plates and allowed to grow under normal growth conditions. Triplicate wells were trypsinized and counted every day using a hemacytometer (Fisher Scientific). Subcutaneous tumor growth was assayed in 6-week old nude mice by injecting 10^6 cells in 0.1ml of serum-free media. Tumor volume was evaluated as described (16). For experimental metastasis, mice received 2×10^6 cells suspended in 0.1 ml of serum-free medium by i.v. lateral tail vein injection as described (16). At the time of euthanasia, the lungs were removed by dissection away from adjacent organs and examined grossly and microscopically. The presence, number, and size of metastatic nodules were scored. Animal experiments were carried out twice or more and results pooled for statistical analysis.

Migration assays

5×10^4 cells were plated onto custom-made glass-bottom 35mm dishes coated with 2μg/ml fibronectin. 5 hours after plating, dishes were transferred to a custom-made heated stage mounted on a Nikon Diaphot-TMD inverted microscope (Nikon Corporation) and imaged every 10 min for 4 hours using a CoolSnap HQ Monochrome camera (Photometrics; Roper Scientific, Inc). Temperature in the medium was maintained at 37°C and pH was controlled by addition of 25mM HEPES buffer. Medium was overlaid with mineral oil to prevent evaporation. Image acquisition was controlled by ISee software (Inovision Corporation). Tracks of individual cells were analyzed using ImageJ software.

Cell spreading

Cells were detached with trypsin-EDTA, pelleted, resuspended in growth medium and replated on glass coverslips coated with 5μg/ml fibronectin. After 4h, cells were fixed with 3.7% formaldehyde and surface area of individual GFP-positive cells was measured using ImageJ software.

RESULTS

The major function of GDI1 is thought to be inhibition of membrane targeting of Rho GTPases (12). To gain insight into the mechanism of metastasis suppression by GDI2, we performed a comparative analysis of GDI1 and GDI2 in regulating the classical Rho GTPases Rac1, Cdc42 and RhoA. We therefore established stable polyclonal cell lines that over-express GFP or GFP fusions with GDI1 and GDI2 (Fig. 1A). Highly metastatic UMUC3 cells that have undetectable levels of endogenous RhoGDI2 (17) were used for these studies. Immunoblotting with a RhoGDI1-specific antibody revealed that the exogenous protein was present at similar levels to endogenous RhoGDI1, thus, total levels increased about 2-fold. Western blotting for GFP showed that overexpressed GFP-GDI1 and GFP-GDI2 were present at similar levels (Fig. 1A). GDI1 over-expression greatly decreased Rac targeting to the membrane fraction (80%), whereas comparable expression of GDI2 had a much smaller effect (40%; Fig. 1B). This result is consistent with the weaker binding of GDI2 to Rho GTPases (18).

To assess functional relevance, we compared the effect of transiently expressed GDI1 and GDI2 on cell spreading, which is highly dependent on Rac and Cdc42 (19). GDI1 strongly inhibited cell spreading whereas effects of GDI2 were negligible (Fig. 1C).

As a complementary approach, we expressed short hairpin RNAs directed against GDI1 and GDI2 in non-metastatic T24 cells that express both GDI1 and GDI2 (1). Two independent stable clones (clone 1 and 3) that exhibited approximately 50% down-regulation of GDI1 were isolated, while GDI2 levels were unaffected (Fig. 2A, upper panel). Conversely, three independent clones (13,15 and 17) showed significant GDI2 depletion without affecting GDI1 (Fig. 2A, lower panel). GDI2 was reduced by ~70% in clones 13 and 15, and was undetectable in clone 17. These cells were fractionated and membrane and cytosol preparations were probed for Rac1, Cdc42 and RhoA. Down-regulation of GDI1 resulted in a 6–9 fold increase in the ratio of membrane to cytosolic Rac1, RhoA and Cdc42 (Figures 2B and 2C). By contrast, reduction of GDI2 had no detectable effect. To analyze cellular functions, we assayed these clones for random migration. As expected, GDI1 depletion increased migration speed 3 to 5-fold (Figures 2D and 2E), however, down-regulation of GDI2 had no effect. Thus, both over-expression and down-regulation show that inhibition of GTPase function by GDI2 ranges from weak to undetectable.

As shown below, GDI2 is a stronger inhibitor of metastasis compared to GDI1 (Fig. 4). These results therefore raise the question whether GDI2 suppresses metastasis through Rho GTPases at all. To address this issue, we took advantage of work that identified residue I177 in GDI1, which corresponds to N174 in GDI2, as an important determinant of their differential affinity for Rho GTPases (18). We made a point mutant in GDI2, N174I, that increases its affinity for Rho GTPases; another mutation in GDI2 (D182R) that decreases its binding (20,21); and a mutation in GDI1 (I177N) that decreases binding to GTPases. Stable cell lines that express GFP fusions of these mutants were established and shown to express at levels similar to their wild type counterparts (Figure 1A and Figure 3).

We next verified that these mutations affect binding to Rho GTPases in the predicted way. We focused on Rac1 because co-immunoprecipitation experiments showed that GDI2 binds mainly to Rac1, whereas binding to Rac2, Rac3, Cdc42, RhoA or RhoC are very weak (Wu and

Theodorescu; submitted). First, the stable cell lines expressing GFP-GDIs were transfected with FLAG-Rac1; the cell lysates were precipitated with anti-FLAG and the amount of bound GFP-RhoGDIs assessed. I177N GDI1 bound poorly to FLAG-Rac1 compared to its wt counterpart; N174I GDI2 showed increased binding compared to wt GDI2; and D182R GDI2 showed essentially no binding to Rac1 (Fig. 3). To examine functional correlates, we again assayed Rac membrane targeting and cell spreading. Wt GDI1 was the most effective inhibitor of Rac function but this was decreased by the I177N mutation (Figures 1B and C). N174I GDI2 inhibited Rac membrane binding and cell spreading modestly but significantly more efficiently than wt GDI2. D182R RhoGDI2 had essentially no effect on Rac function. Thus, these constructs behaved as expected.

Next, we analyzed growth of these stable cell lines. In tissue culture, growth of the GDI1 cell line was moderately slower than control GFP-expressing cells. The D182R GDI2 and I177N GDI1 lines grew moderately faster, and other lines grew similarly to control (Fig. 4A). When injected subcutaneously into mice, these lines showed similar behavior: the GDI1 tumors grew slower, whereas the D182R GDI2 and I177N GDI1 tumors grew faster than the control GFP line, with others growing at similar rates to control (Fig. 4B).

Next, we examined their behavior in the experimental metastasis model. Cells were injected via tail veins and lung metastases monitored (Table I). GDI2 significantly reduced both the percentage of mice with metastatic nodules in the lungs (48% with GFP compared to 6.6% with GFP-GDI2) and the number of tumors in the tumor-bearing mice. Thus, the total tumor burden decreased by approximately 15-fold. GDI1 expression moderately reduced the incidence of metastasis (26.6%), however, this reduction correlates with the slower growth of these cells (Figure 4A and Figure 4B). I177N GDI1 showed both faster growth and a corresponding increase in metastases. Surprisingly, the GDI2 mutants with either higher or lower affinity for Rho GTPases lost their ability to inhibit metastases. Therefore, suppression of metastasis is specific to wt RhoGDI2 and cannot be attributed to general reduction of growth rates.

These results suggest that RhoGDI2 inhibits metastasis through Rho GTPases, however, this effect cannot be mediated by inhibition of GTPase function. An alternative mechanism is based on the fact that Rac, Rho and Cdc42 each have many effectors and some effector pathways inhibit migration and invasion (22,23). Interestingly, our previous work also implicated GDI1 in the activation mechanism for Rac (12). Thus, it seems possible that GDI2 might direct activity of a Rho GTPase toward a specific pathway that inhibits metastasis. Given that GDI2 has the highest affinity for Rac1, this GTPase is the main candidate. However, the general importance of Rac1 in metastasis precludes testing this idea using the experimental metastasis model by globally inhibiting Rac1. But as a first step, we were able to assess effects of RhoGDI constructs on Rac1 activity. Pull-down assays with the PAK effector domain were done using the cells expressing GFP, GFP-RhoGDI1 or GFP-RhoGDI2. GDI1 cells showed a decrease in Rac1 activity, as expected, whereas GDI2 over-expression consistently increased Rac1 activity compared to control GFP cells (Fig. 5A). Conversely, when knock-down lines were examined, clone 17 that had undetectable levels of GDI2 showed reduced Rac1 activity (Fig. 5B). Clones 13 and 15 did not show similar reductions, most likely because knock-down of GDI2 was less efficient. To examine this issue in more detail, effects of the point mutants on Rac1 activity were examined. Both N174I and D182R RhoGDI2 failed to affect Rac1 activation, while the I177N GDI1 construct lost its ability to inhibit Rac1 (Fig. 5A). Thus, metastasis suppression correlates with increased rather than decreased Rac1 activity.

To test whether elevated Rac activity is accompanied by changes in cytoskeletal architecture, F-actin and vinculin containing adhesions were visualized in spreading cells. However, elevated Rac in GDI2 cells did not cause obvious increases in actin-rich protrusions or

membrane ruffling (Supplementary Figures 1 and 2). We also investigated pathways downstream of Rac that might mediate metastasis suppression. We first assayed activity of SAPK/JNK and PAK, however, no correlation was observed between activation of these pathways and metastatic potential (Supplemental Figure 3). We also considered whether Rac1 suppresses metastasis through inhibition of RhoA. GST-Rhotekin RBD pull-down assays (Figure 5C) showed no change in RhoA activity in cells expressing GDI1 or GDI2. We have not been able to conclusively measure RhoC activation, most likely due to low expression (data not shown). Thus, suppression of metastasis correlates with elevated Rac activity but not with activation of known Rac downstream pathways currently implicated in cancer.

DISCUSSION

In this study, we set out to investigate the mechanism by which RhoGDI2 suppresses metastasis. Our results show that GDI1 and GDI2 are functionally distinct. Specifically, RhoGDI1 is a strong negative regulator of Rho GTPases, which correlates with the strength of GDI1 binding to GTPases. In contrast, GDI2 inhibits GTPase function weakly if at all, yet strongly inhibits metastasis. Surprisingly, mutations that either increase or decrease the affinity of GDI2 for GTPases both abolish metastasis. These data provide strong evidence that GDI2 acts via a distinct mechanism from GDI1 and that it does not do so by inhibiting GTPase activity or function.

On the contrary, metastasis suppression correlated with increased Rac1 activity. At first glance, this result might seem to conflict with the slight increase in cytoplasmic Rac1 in the GDI2 over-expressing cells. However, GDI1 binds GTP-loaded Rac1 and can sequester V12 mutants in the cytoplasm (24). Therefore, the combination of moderate activation of Rac1 with weak inhibition of Rac1 membrane targeting is consistent with the complete absence of any detectable inhibition of Rac1 function.

The mutational studies suggest that metastasis suppression involves Rho GTPases but the blockade by both increased and decreased affinity shows that the effect involves a highly precise relationship. This situation is reminiscent of systems where mutations that either inhibit or constitutively activate GTPases or protein phosphorylation both block function of the proteins (25,26). The usual interpretation is that both types of mutations inhibit kinetic processes that involve cycling between two (or more) states. These results further support the conclusion that RhoGDI2 inhibits metastasis through a mechanism distinct from simple blockade of GTPase function.

We can at present only speculate what that mechanism might be. Available evidence suggests that GDI2 binds with highest affinity to Rac1 (Wu and Theodorescu; submitted). Interestingly, there is also precedent for the idea that Rac1 can act in a pathway that suppresses metastasis (22,23). In this study, activation of Rac1 through its GEF TIAM1 specifically induced cohesion of epithelial colonies and suppressed migration and invasion. GEFs for Rho GTPases have in several cases been found to scaffold specific effectors, thereby directing GTPase activation toward specific downstream pathways (27). Although we do not see increased cell-cell adhesion in GDI2-expressing cell lines, many pathways downstream of Rac1 have been identified, one or more of which might also suppress metastatic growth. This general notion is also consistent with results that implicate GDI1 in activation of Rac1 (12). Activation of JNK or inhibition of Rho are possible pathways for metastasis suppression (28,29); we also examined PAK as an important Rac effector. However, our current data do not support their involvement in metastasis expression. Indeed, the failure to see elevated ruffling, JNK or PAK activity in cells with higher Rac activity supports the idea that GDI2 specifically targets Rac toward a novel effector pathway. Taken together, these results support the idea that Rac is specifically directed toward a distinct downstream pathway.

These considerations lead us to the hypothesis that GDI2 might promote interaction of Rac1 with a specific GEF to induce activation of Rac1 through a pathway that inhibits metastasis. Mutations that either increase or decrease the affinity of GDI2 for Rac1 could inhibit this pathway, since either one would decrease the rate of the reaction in which Rac1 is transferred from GDI2 to the GEF; decreased affinity would prevent the initial targeting of the GTPase while increased affinity would allow targeting but prevent dissociation of GDI and thus activation of the GTPase.

In conclusion, these data demonstrate the RhoGDI2 suppresses metastasis through a mechanism that is not shared with GDI1 and that is not dependent on simple inhibition of Rho GTPases. The data can be explained if GDI2 specifically directs Rac toward an effector pathway that inhibits metastatic migration or growth. However, experimental testing of this must await identification of the components of this pathway and will be the focus of future work.

Supplementary Material

Refer to Web version on PubMed Central for supplementary material.

ACKNOWLEDGEMENTS

This work was supported by NIH grant R01 GM47214 to M.A.S. and NIH grant CA104106 to D.T.

REFERENCES

1. Gildea JJ, Seraj MJ, Oxford G, Harding MA, Hampton GM, Moskaluk CA, Frierson HF, Conaway MR, Theodorescu D. RhoGDI2 is an invasion and metastasis suppressor gene in human cancer. Cancer Res 2002;62:6418–6423. [PubMed: 12438227]
2. Harding MA, Theodorescu D. RhoGDI2: a new metastasis suppressor gene: discovery and clinical translation. Urol Oncol 2007;25:401–406. [PubMed: 17826660]
3. Olofsson B. Rho guanine dissociation inhibitors: pivotal molecules in cellular signalling. Cell Signal 1999;11:545–554. [PubMed: 10433515]
4. DerMardirossian C, Bokoch GM. GDIs: central regulatory molecules in Rho GTPase activation. Trends Cell Biol 2005;15:356–363. [PubMed: 15921909]
5. Theodorescu D, Sapinoso LM, Conaway MR, Oxford G, Hampton GM, Frierson HF Jr. Reduced expression of metastasis suppressor RhoGDI2 is associated with decreased survival for patients with bladder cancer. Clin Cancer Res 2004;10:3800–3806. [PubMed: 15173088]
6. Dransart E, Olofsson B, Cherfils J. RhoGDIs revisited: novel roles in Rho regulation. Traffic 2005;6:957–966. [PubMed: 16190977]
7. Van Aelst L, D'Souza-Schorey C. Rho GTPases and signaling networks. Genes Dev 1997;11:2295–2322. [PubMed: 9308960]
8. Miura Y, Kikuchi A, Musha T, Kuroda S, Yaku H, Sasaki T, Takai Y. Regulation of morphology by rho p21 and its inhibitory GDP/GTP exchange protein (rho GDI) in Swiss 3T3 cells. J Biol Chem 1993;268:510–515. [PubMed: 8416955]
9. Takaishi K, Kikuchi A, Kuroda S, Kotani K, Sasaki T, Takai Y. Involvement of rho p21 and its inhibitory GDP/GTP exchange protein (rho GDI) in cell motility. Mol Cell Biol 1993;13:72–79. [PubMed: 8417362]
10. Takaishi K, Sasaki T, Kato M, Yamochi W, Kuroda S, Nakamura T, Takeichi M, Takai Y. Involvement of Rho p21 small GTP-binding protein and its regulator in the HGF-induced cell motility. Oncogene 1994;9:273–279. [PubMed: 8302589]
11. Michaelson D, Silletti J, Murphy G, D'Eustachio P, Rush M, Philips MR. Differential localization of Rho GTPases in live cells: regulation by hypervariable regions and RhoGDI binding. J Cell Biol 2001;152:111–126. [PubMed: 11149925]

12. Moissoglu K, Slepchenko BM, Meller N, Horwitz AF, Schwartz MA. In vivo dynamics of Rac-membrane interactions. Mol Biol Cell 2006;17:2770–2779. [PubMed: 16597700]

13. Ishizaki H, Togawa A, Tanaka-Okamoto M, Hori K, Nishimura M, Hamaguchi A, Imai T, Takai Y, Miyoshi J. Defective chemokine-directed lymphocyte migration and development in the absence of Rho guanosine diphosphate-dissociation inhibitors alpha and beta. J Immunol 2006;177:8512–8521. [PubMed: 17142749]

14. Gorovoy M, Neamu R, Niu J, Vogel S, Predescu D, Miyoshi J, Takai Y, Kini V, Mehta D, Malik AB, Voyno-Yasenetskaya T. RhoGDI-1 modulation of the activity of monomeric RhoGTPase RhoA regulates endothelial barrier function in mouse lungs. Circ Res 2007;101:50–58. [PubMed: 17525371]

15. Morgenstern JP, Land H. Advanced mammalian gene transfer: high titre retroviral vectors with multiple drug selection markers and a complementary helper-free packaging cell line. Nucleic Acids Res 1990;18:3587–3596. [PubMed: 2194165]

16. Seraj MJ, Harding MA, Gildea JJ, Welch DR, Theodorescu D. The relationship of BRMS1 and RhoGDI2 gene expression to metastatic potential in lineage related human bladder cancer cell lines. Clin Exp Metastasis 2000;18:519–525. [PubMed: 11592309]

17. Titus B, Frierson HF Jr, Conaway M, Ching K, Guise T, Chirgwin J, Hampton G, Theodorescu D. Endothelin axis is a target of the lung metastasis suppressor gene RhoGDI2. Cancer Res 2005;65:7320–7327. [PubMed: 16103083]

18. Platko JV, Leonard DA, Adra CN, Shaw RJ, Cerione RA, Lim B. A single residue can modify target-binding affinity and activity of the functional domain of the Rho-subfamily GDP dissociation inhibitors. Proc Natl Acad Sci U S A 1995;92:2974–2978. [PubMed: 7708758]

19. Price LS, Leng J, Schwartz MA, Bokoch GM. Activation of Rac and Cdc42 by integrins mediates cell spreading. Mol Biol Cell 1998;9:1863–1871. [PubMed: 9658176]

20. Gandhi PN, Gibson RM, Tong X, Miyoshi J, Takai Y, Konieczkowski M, Sedor JR, Wilson-Delfosse AL. An activating mutant of Rac1 that fails to interact with Rho GDP-dissociation inhibitor stimulates membrane ruffling in mammalian cells. Biochem J 2004;378:409–419. [PubMed: 14629200]

21. Scheffzek K, Stephan I, Jensen ON, Illenberger D, Gierschik P. The Rac-RhoGDI complex and the structural basis for the regulation of Rho proteins by RhoGDI. Nat Struct Biol 2000;7:122–126. [PubMed: 10655614]

22. Hordijk PL, ten Klooster JP, van der Kammen RA, Michiels F, Oomen LC, Collard JG. Inhibition of invasion of epithelial cells by Tiam1-Rac signaling. Science 1997;278:1464–1466. [PubMed: 9367959]

23. Uhlenbrock K, Eberth A, Herbrand U, Daryab N, Stege P, Meier F, Friedl P, Collard JG, Ahmadian MR. The RacGEF Tiam1 inhibits migration and invasion of metastatic melanoma via a novel adhesive mechanism. J Cell Sci 2004;117:4863–4871. [PubMed: 15340013]

24. Del Pozo MA, Kiosses WB, Alderson NB, Meller N, Hahn KM, Schwartz MA. Integrins regulate GTP-Rac localized effector interactions through dissociation of Rho-GDI. Nat Cell Biol 2002;4:232–239. [PubMed: 11862216]

25. Han J, Rose DM, Woodside DG, Goldfinger LE, Ginsberg MH. Integrin alpha 4 beta 1-dependent T cell migration requires both phosphorylation and dephosphorylation of the alpha 4 cytoplasmic domain to regulate the reversible binding of paxillin. J Biol Chem 2003;278:34845–34853. [PubMed: 12837751]

26. Lin Q, Fuji RN, Yang W, Cerione RA. RhoGDI is required for Cdc42-mediated cellular transformation. Curr Biol 2003;13:1469–1479. [PubMed: 12956948]

27. Buchsbaum RJ. Rho activation at a glance. J Cell Sci 2007;120:1149–1152. [PubMed: 17376960]

28. Itoh K, Yoshioka K, Akedo H, Uehata M, Ishizaki T, Narumiya S. An essential part for Rho-associated kinase in the transcellular invasion of tumor cells. Nat Med 1999;5:221–225. [PubMed: 9930872]

29. Vander Griend DJ, Kocherginsky M, Hickson JA, Stadler WM, Lin A, Rinker-Schaeffer CW. Suppression of metastatic colonization by the context-dependent activation of the c-Jun NH2-terminal kinase kinases JNKK1/MKK4 and MKK7. Cancer Res 2005;65:10984–10991. [PubMed: 16322247]

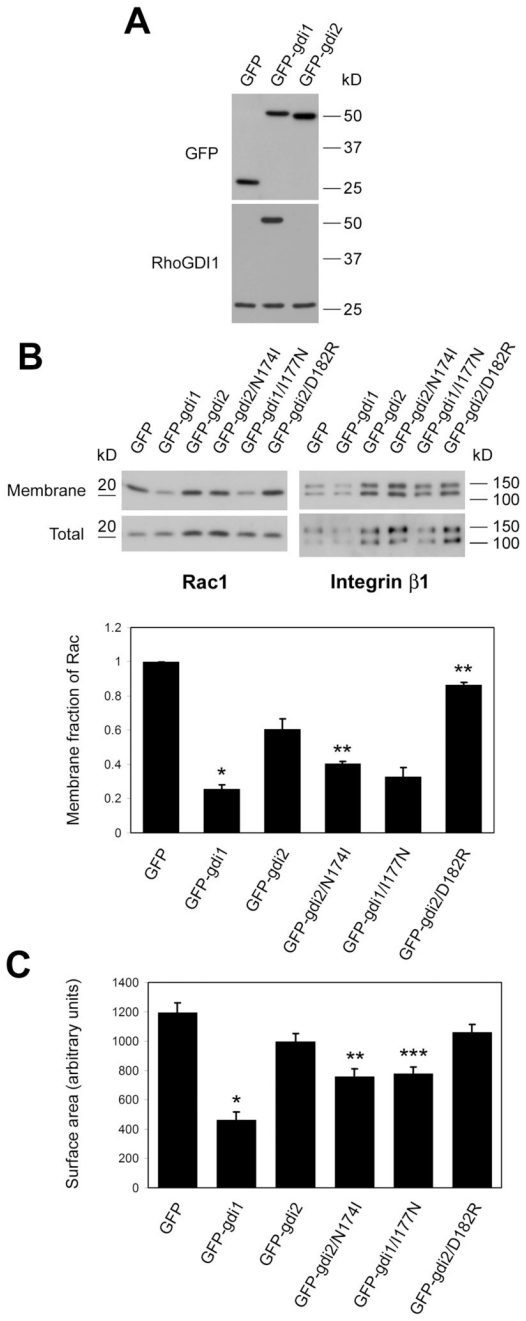

Figure 1. RhoGDI over-expression

(A) Lysates of UMUC3 cells stably expressing GFP, GFP-GDI1 or GFP-GDI2 were resolved by SDS-PAGE and immunoblotted for GFP and RhoGDI1. (B) Membrane fractions and total lysates were immunoblotted for Rac1 and integrin β1. Bar graph: mean ± SEM of membrane/total ratio of Rac1 compared to control cells; n=3. *: $p<0.01$ (compared to GFP-GDI2); **: $p<0.05$ (compared to GFP-GDI2). (C) Surface area of UMUC3 cells expressing the indicated constructs after plating on fibronectin for 4 hours. Values are means ± SEM (n=78-102). *: $p<0.001$ (compared to GFP-GDI2); **: $p<0.005$ (compared to GFP-GDI2); ***: $p<0.001$ (compared to GFP-GDI1). p values were calculated by Student's t-test.

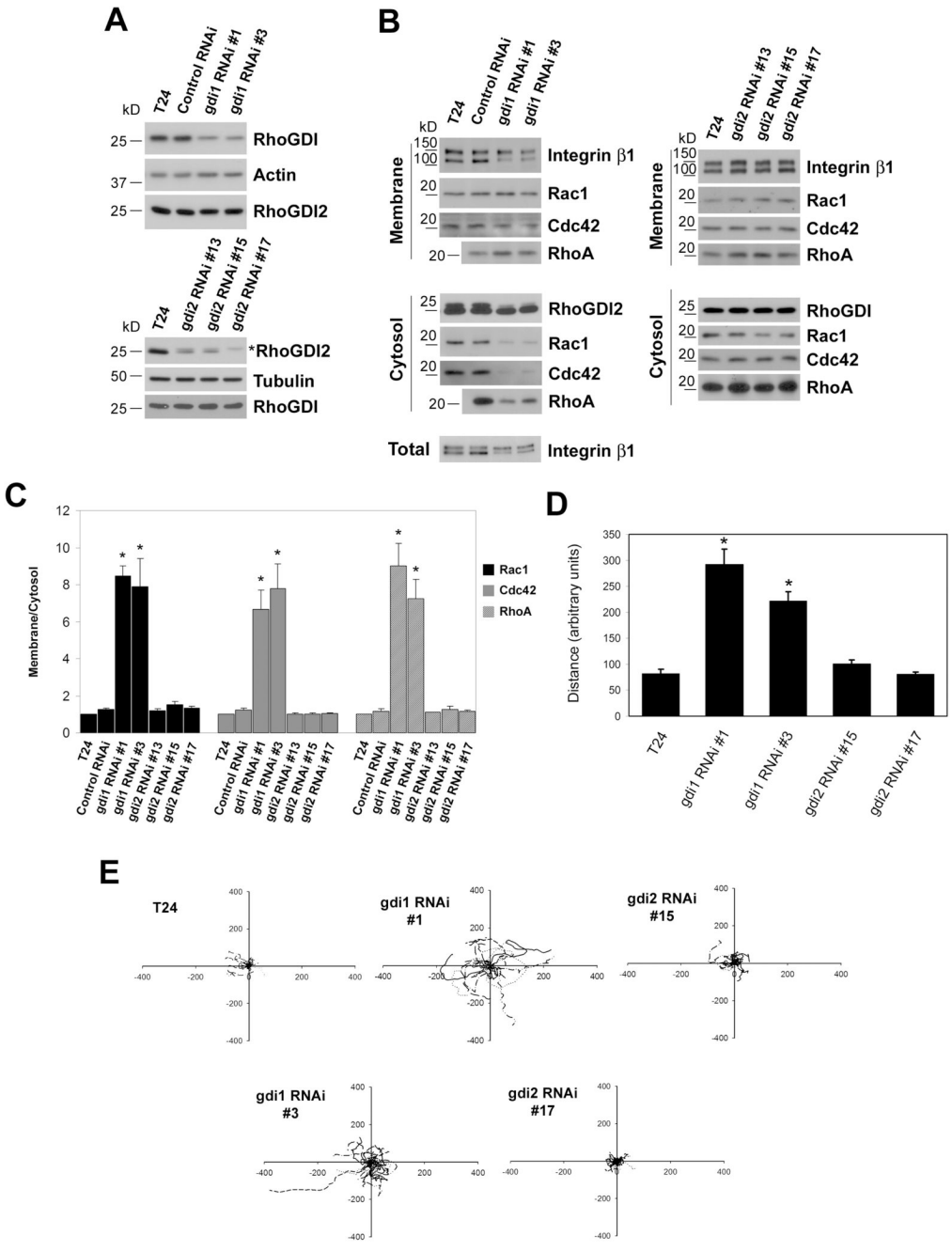

Figure 2. RhoGDI knock-down

(A) Lysates from parental T24 cells and control or RhoGDI1 RNAi clones (upper panel) or RhoGDI2 RNAi clones (lower panel) were resolved by SDS-PAGE and immunoblotted for RhoGDI1, RhoGDI2, actin and tubulin. Asterisk in the lower panel denotes cross-reactivity of the antibody with RhoGDI1. RhoGDI2 corresponds to the lower band. (B) Equal percentages of cytosolic and membrane fractions were resolved by SDS-PAGE and immunoblotted for Rac1, Cdc42, and RhoA. Integrin β1 and RhoGDI1 or RhoGDI2 were used as membrane and cytosol markers, respectively. (C) Quantification of membrane/cytosol ratios from B. Values are means ± SEM (n=3). *: $p<0.05$ (compared to the corresponding control RNAi). (D) Quantification of distance migrated for the indicated cell types shown in E. Values are means

± SEM, n=19–34. *: p<0.001 (compared to T24). (E) Representative migrations tracks. The origin of all tracks was arbitrarily set to coordinates [0, 0].

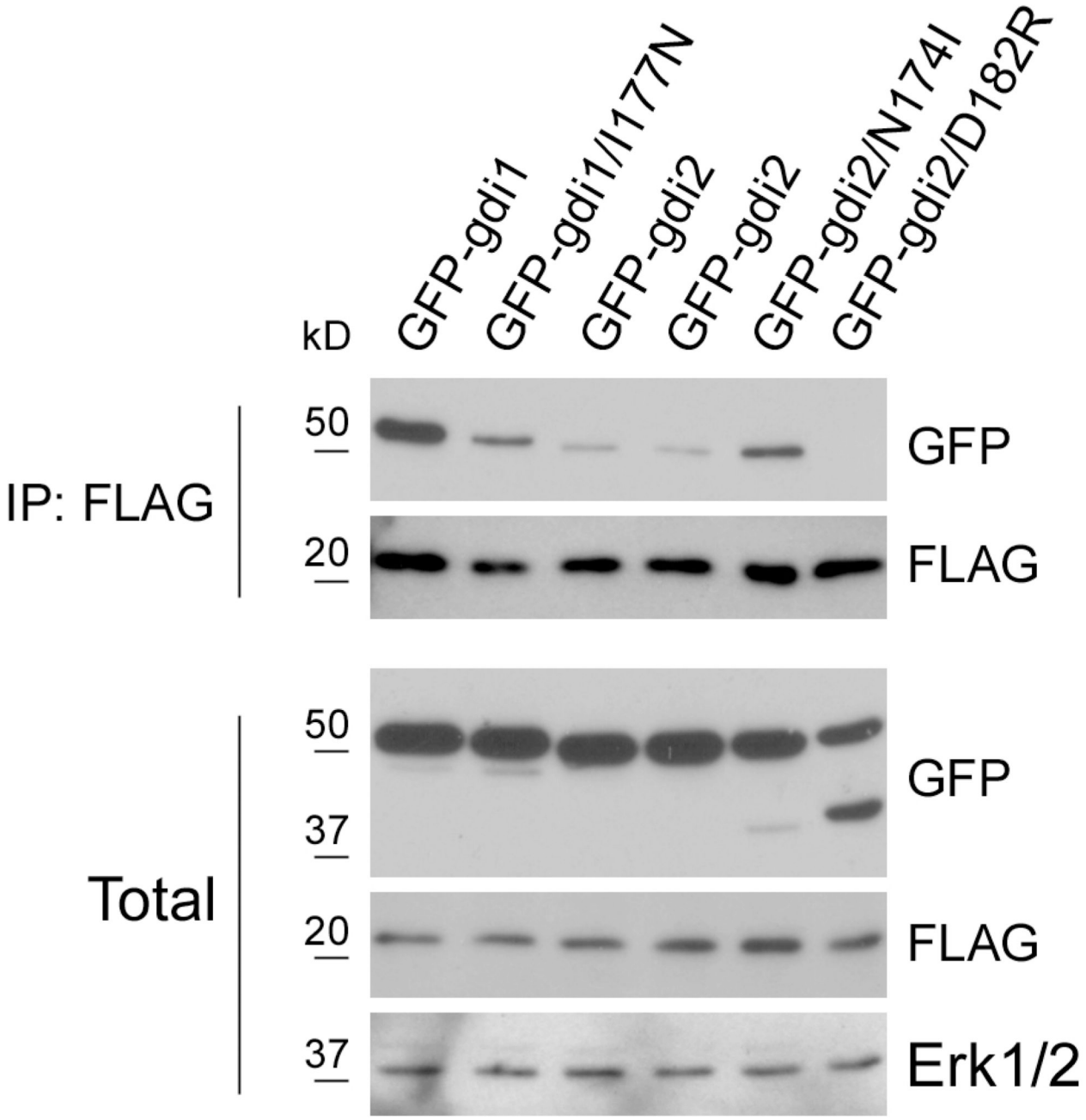

Figure 3. Characterizing GDI1 and GDI2 mutants

Lysates of the indicated stable UMUC3 lines transfected with FLAG-Rac were subjected to immunoprecipitation with anti-FLAG and samples analyzed by immunoblotting for GFP and FLAG. Anti-Erk1/2 was used as a loading control. Data are representative of three independent experiments.

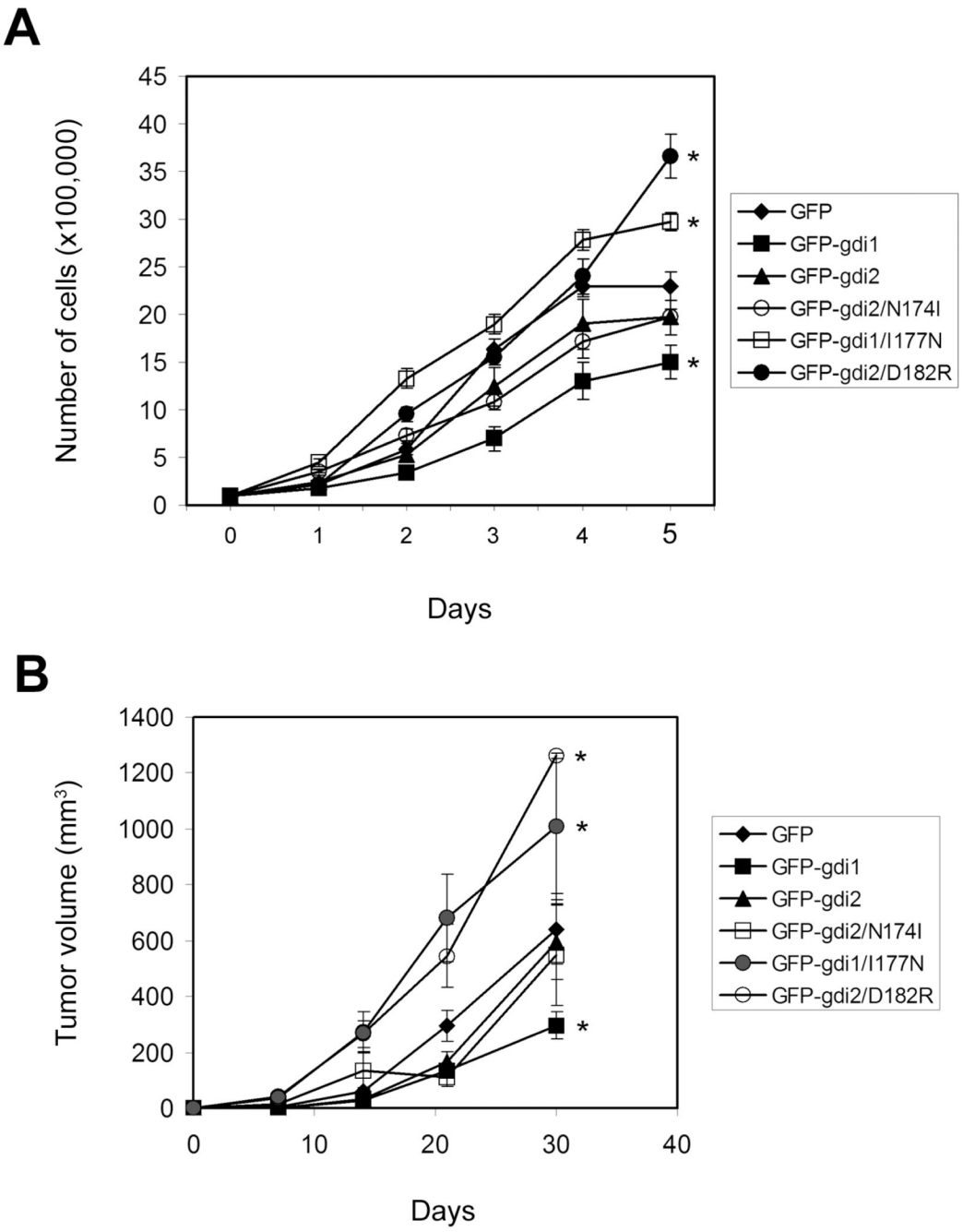

Figure 4. Growth of RhoGDI cell lines

(A) In vitro growth of the indicated stable cell lines. Values are means ± SEM (n=3). *: $p<0.03$ compared to control cells (GFP), by Student's t-test. (B) Subcutaneous growth in nude mice. Values (tumor volumes) are means ± SEM (n=7–10). *: $p<0.05$ compared to control cells (GFP), by Student's t-test. Experiments were performed in duplicate on separate occasions with similar results.

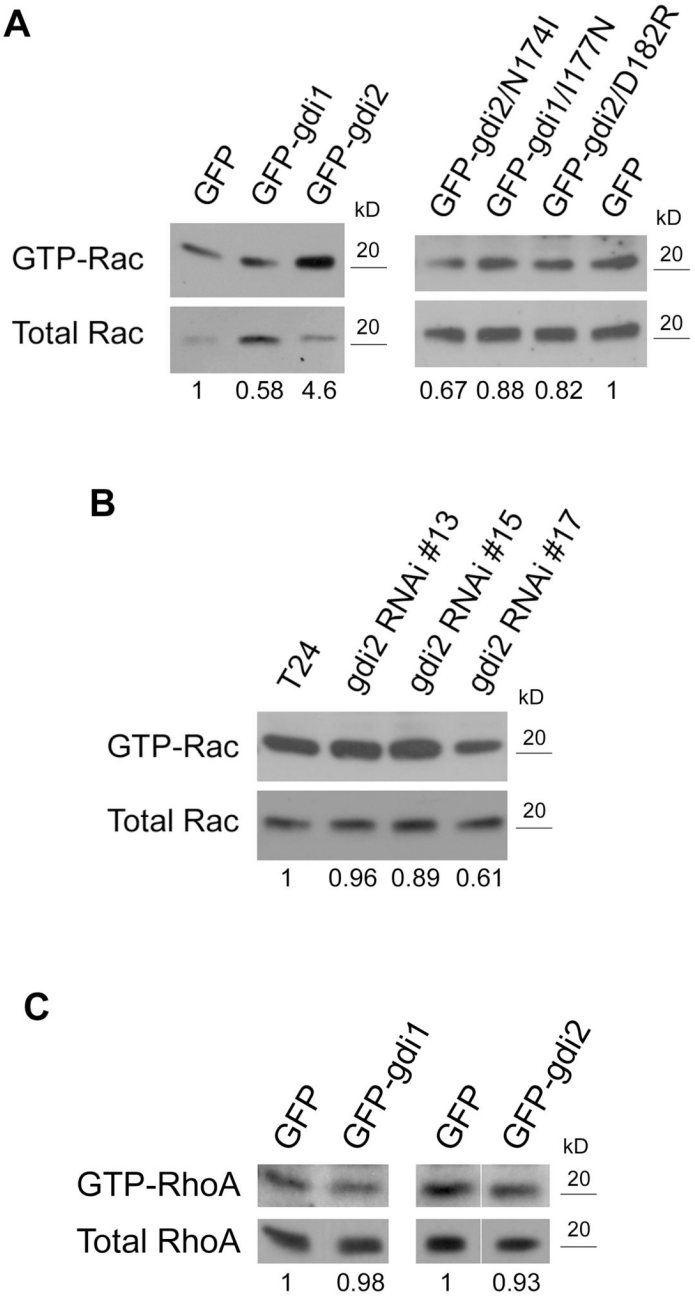

Figure 5. RhoGDI2 increases Rac activity

GST-PBD and GST-RBD pull down assays were carried out using lysates from the indicated stably over-expressing (A and C) or stable knock-down cell lines (B). Numbers represent the ratio of active /total Rac or RhoA relative to control cells (GFP in A and C, T24 in B); n=3. In C, the GDI2 lane is shown with the GFP lane from different parts of the same gel.

Table I

Effect of GDIs on experimental metastasis

Cell line	Number of mice	% of mice with metastases	Average number of metastases (in metastasis-bearing mice)†	Average number of metastases (in total number of mice) †
GFP	25	48	3.75±0.59	1.8±0.28
GFP-gdi1	15	26.6	3.75±1.1	0.99±0.29
GFP-gdi2	15	6.6§	2¶	0.13
GFP-gdi2/N174I	20	20	7.25±2.5	1.45±0.5
GFP-gdi1/I177N	20	50	5.2±2.2	2.6±1.1
GFP-gdi2/D182R	20	55	9.18±4.13	5.04±2.27

Data were pooled from two independent experiments with consistent results. Mice were sacrificed 12 weeks post injection.

† Values are means ± SEM.

§ $p<0.01$ by chi-square test (compared to GFP).

¶ $p<0.02$ by Student's t-test (compared to GFP).